*Sādhanā* (2024)49:97
https://doi.org/10.1007/s12046-024-02442-x


# Regenerative instabilities in guided metal circular sawing

SUNNY SINGHANIA[1,2] and MOHIT LAW[1,*]

[1]Machine Tool Dynamics Laboratory, Department of Mechanical Engineering, Indian Institute of Technology Kanpur, Kanpur, Uttar Pradesh 208016, India
[2]Department of Foundry and Forge technology, National Institute of Advanced Manufacturing Technology (formerly NIFFT), Ranchi, Jharkhand 834003, India
e-mail: mlaw@iitk.ac.in

MS received 28 June 2023; revised 3 December 2023; accepted 8 December 2023

**Abstract.** This paper reports on new research that: characterizes the influence of regenerative lateral forces on the stability of metal circular sawing; describes the role of process damping in potentially stabilizing the sawing process; and investigates the role that distributed and lubricated guides play in a sawing process prone to regenerative instabilities. We model the saw as a rotating disc using the Von Kármán plate theory. Equations of motion are derived using the Hamilton's principle. Guides are modelled as being distributed and properties of the fluid are modelled to be a function of the guide size and its placement relative to the saw. The regenerative and process damping effects are incorporated based on other similar models for milling processes. Our model-based analysis suggests that: regenerative instabilities are characterized by a growth in the real part of the eigenvalue of the system; clearance between the guide and the rotating saw and the guide's circumferential placement with respect to the cutting zone both influence the severity and speed regions of instabilities; material being cut and changing cutting engagements do not significantly influence the region of instabilities; and that process damping can help stabilize an otherwise unstable process. Though models need to be validated, our observations can still instruct the design of stable guided metal sawing processes in industries.

**Keywords.** Circular sawing; chatter; regeneration; process damping; dynamics.

## 1. Introduction

Metal cutting circular saws that rotate at low speeds are fed into bars and tubes to part them to length. To minimize work material losses, saws are made thin. Their thinness makes them vibrate when excited by the cutting process. Every vibrating tooth on the saw leaves its imprint on the side walls of the workpiece due to flank cutting. When there is a phase difference between such waves left by successive teeth in cut, vibration amplitudes can modulate and grow to result in self-excited type regenerative chatter vibration instabilities. Chatter, if not avoided, will damage workpiece machined surface quality. Chatter may also result in tool breakage and may damage elements of the sawing machine. It is hence important to characterize chatter in metal circular sawing. Doing so forms the focus of this paper.

The focus of this paper is primarily on regenerative chatter, and not so much on critical speed related, buckling, and/or flutter instabilities that are also reported to occur in sawing processes, especially in the sawing of wood. Metal sawing, as opposed to sawing of wood, is a low-speed process [1, 2]. Buckling related instabilities and flutter instabilities occur at speeds higher than critical, and critical speeds occur at speeds higher than the low-speed regime of interest herein. Hence the focus herein remains on regenerative instabilities that may occur at low cutting speeds.

Unlike other machining processes such as turning and milling wherein the main tangential and/or feed forces are responsible for chatter, circular sawing is characterized by significant flank cutting that is responsible for chatter. And, unlike turning and milling processes that have been studied in some detail [3–5], there is no significant literature characterizing regenerative instabilities in metal circular sawing. Though there is some relevant research reported in [6, 7], those reports were concerned with sawing of wood that occurs at much higher speeds than the metal sawing of interest herein. Some limited experimental investigations on metal circular sawing were reported in [8], and some preliminary model-based investigations limited to approximating a distributed guide as a point guide were reported in our own prior work [9, 10]. It is hence the main aim of this paper to contribute to a nuanced understanding of the main factors influencing chatter due to flank cutting in circular sawing.

Moreover, because of interference between the saw tooth's flank face and the wall of the machined surface

*For correspondence
Published online: 05 March 2024

during relative transverse vibrations between the saw and the workpiece there is a dissipation of energy caused by the machining process itself that is referred to as process damping. This energy dissipation is known to be a low-speed phenomena, i.e., the speed regime of interest in metal circular sawing. Though extensive research has been conducted in this direction for turning and milling [11–16], since process damping in sawing is unlike that in milling and/or turning, those studies and their inferences are not of direct relevance to sawing. In turning and milling, the interaction of the cut surface with the tool's flank face is usually in the feed direction. Whereas in sawing, the interaction is along the lateral direction, i.e., in the direction normal to the feed direction. Since there exists no research characterising the role of process damping in potentially stabilizing the sawing process in the presence of regenerative instabilities, doing so forms another aim of this paper.

Furthermore, because saws are thin and prone to vibrations in their lateral direction, saws are usually guided by multiple pairs of stationary and distributed guides placed on either side of the rotating saw. Guides placed at some distance away from the saw provide bearing surfaces to arrest large out-of-plane vibrations. Usually, there is a fluid in between the guide and the saw that can be air, oil, an oil emulsion, or grease. The fluid helps reduce friction between the swarf and the saw tooth, cool the saw and the cutting region, and sometimes flush away the swarf from the cutting region. Depending on the fluid in use, lubricated guides can provide varying levels of additional stiffness, mass, damping, and affect the viscous shear on the saw. Though there has been extensive research to characterize the role of guides on the critical speed related instabilities of circular saws [2, 17–19], what role, if any, do distributed and lubricated guides play if/when the sawing process is prone to regenerative instabilities is not known, and this forms yet another major focus of this paper.

Since the saw's geometry, its boundary conditions, its initial stress-state, its speed of rotation, the size and the number of guide pads being used, their location relative to the cutting region, the properties of fluid media between the saw and the guide, the distance of guides from the saw, the engagement conditions, the properties of workpiece material being cut, the process damping effect, and the number of teeth in cut—may each govern the dynamics and stress-stability relationship of the system, and since such analysis for metal circular sawing remains unexplored in previous research, this paper summarizes original research aimed at filling those research gaps. And, since the experimental try-and-see approach is prohibitive and expensive since experiments to test for regenerative instability mechanisms can be destructive and damage parts of the equipment, this paper adopts model-based investigations that incorporates all major influences on the saw vibrational response.

The three main aims of this paper are to report on research that: (i) characterizes the influence of regenerative lateral forces on the stability of metal circular sawing, (ii) describes the role of process damping in potentially stabilizing the sawing process, and (iii) investigates the role that distributed and lubricated guides play in a sawing process prone to regenerative instabilities. Such analysis as is presented in this paper is new and is our modest contribution to the state-of-the-art in understanding instabilities in metal circular sawing processes.

The remainder of the paper is structured as follows. We first present a model for the sawing process. The saw is modelled as a rotating disc using the Von Kármán plate theory. The governing equations of motion are derived using the extended Hamilton's principle. Guides are modelled as being distributed. The properties of the fluid are modelled to be a function of the guide size and its placement relative to the saw. The model includes damping internal to the saw and due to the process. The model builds on well-established models for circular sawing [2, 6–10, 17–19]. The regenerative effect is incorporated based on other similar models for milling processes [6, 7, 20]. And the process damping effect is incorporated based on models reported in [13, 14]. To solve for the regenerative forced vibration response that involves a system of delay differential equations, we use a Fourier series expansion [20] and employ the Muller method with deflation [21] to find the roots of the resulting characteristic equation. These aspects are discussed in the modelling section of the paper. The section after presents parametric model-based numerical analysis to characterize the regenerative instabilities being influenced by of the size of the guides, their location with respect to the cutting region and the saw, changing engagement conditions and workpiece material, and process damping. Discussions and prescriptions for avoiding instabilities follow with the main conclusions.

## 2. Model for a guided circular saw subjected to regenerative and process damping forces

This section presents the governing equations of motion for a lubricated guided saw subjected to multiple moving lateral regenerative cutting forces caused by flank cutting. A model for process damping due to flank rubbing is also presented. The saw is modelled as an annular circular disk of clamped inner radius $b$, free outer radius $a$, and thickness $h$, rotating at a constant angular velocity $\Omega$ in the counter-clockwise direction. The saw is cutting a solid bar with an instantaneous entry angle, $\gamma_{st}$ and the corresponding exit angle, $\gamma_{ex}$ as shown in figure 1. The circular saw is laterally constrained by a lubricated guide pad pair on both sides placed at some distance from the surface of saw. The guides are assumed to be fixed independently on the machine frame. These guides are placed circumferentially between $\gamma_1$ and $\gamma_2$ with their inner and outer radii being $r_1$ and $r_2$, respectively. The schematic in figure 1(a) shows two guides

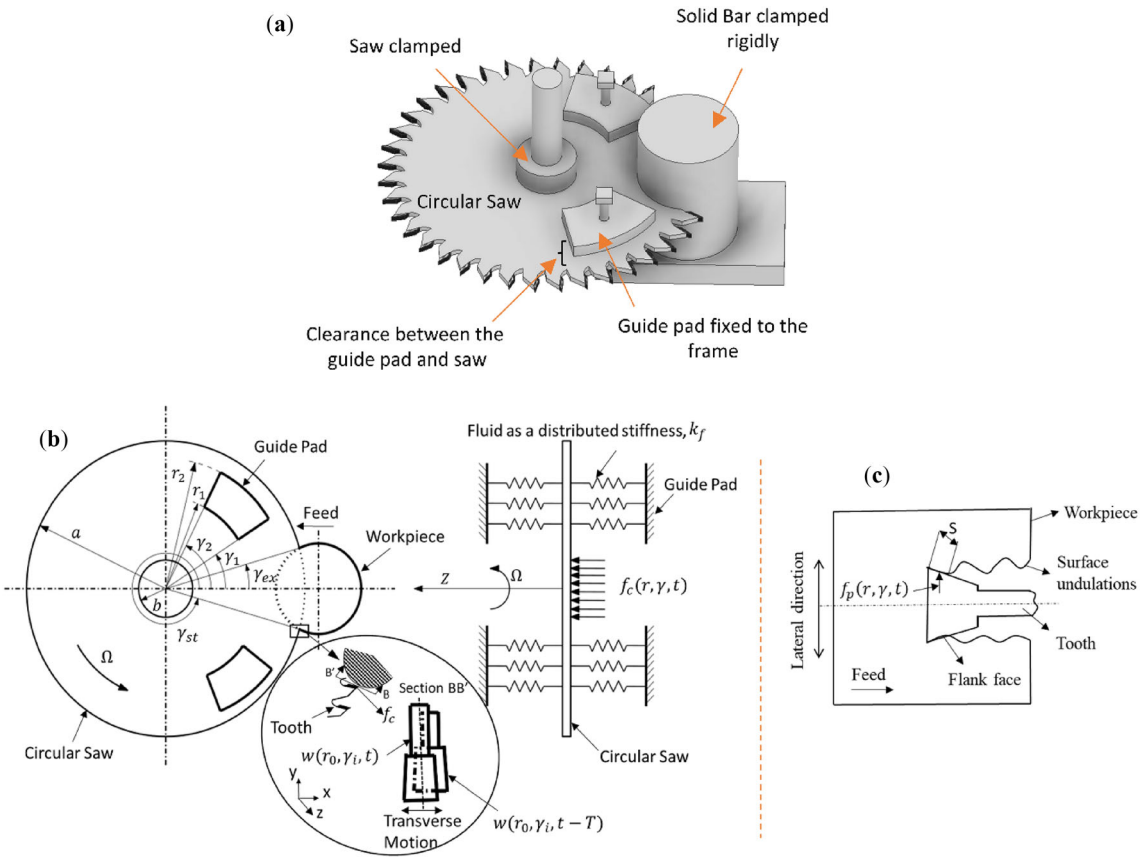


**Figure 1.** **(a)** 3D CAD schematic of the circular saw constrained by guides and cutting a bar. (**b**) Schematic showing a circular saw subjected to lateral regenerative cutting forces constrained with distributed and lubricating guide, (**c**) process damping force acting on a saw tooth.

placed symmetrically with respect to cutting zone. However, the model is generalized to account for more guide pad pairs. And since prior work has shown that the fluid's mass and damping play a negligible role [2], the fluid interaction between the guide pad and the saw is modelled as distributed fluid stiffness.

The regenerative forces that act on the saw are shown schematically in figure 1(b). These forces are superposed with the forces due to the fluid's interaction with the saw, and due to flank rubbing resulting in process damping. While considering regeneration, we neglect the in-plane radial and tangential forces and assume that only the lateral regenerative cutting force, $f_c(t)$, makes the saw vibrate in the transverse direction. This force is assumed to be a linear function of relative tooth displacement. This is evident from the section BB' in figure 1(b), wherein the regenerative effect is associated with an extra lateral cutting area between two successive teeth associated with the transverse response $w(r_o, \gamma_i, t)$ of the current tooth (the ith tooth) and the transverse response $w(r_o, \gamma_i, t-T)$ of the previous tooth (the (i-1)th tooth) at a given location $(r_o, \gamma_i)$ of the workpiece [20]. $T = 2\pi/(\Omega N_t)$ is the tooth passing period, i.e., the period between two successive teeth coming into cut—also called the delay. $N_t$ are the number of teeth.

For the process damping force, $f_c(t)$, we postulate that the lateral force on the saw's flank face acts against the saw-workpiece relative vibration velocity. This interaction is thought to result in friction between the saw's flank face and the previously cut surface, which in turn may contribute to process damping in the system. The rubbing action between the saw tooth's flank face and the vibration marks left by the previous tooth is shown schematically in figure 1c, wherein $S$ is the length of contact of the flank face of the tooth with the machined surface.

Since the saw is thin and vibrations are expected to be of less than the saw's thickness, we use the Von Kármán plate theory and Kirchhoff's plate theory hypothesis to develop an analytical model. Alongside the usual assumptions that go with these theories, we also assume that the saw is made of a viscoelastic material with an internal damping force proportional to the strain rate, and that the saw's expected vibration is smaller than the thickness of the fluid film, and hence the pressure variations across the fluid film thickness are negligible. We further assume that the stiffness of the

fluid is a function of the fluid properties and of the size of the guide. Additionally, we assume that the clearances between the guides and the saw do not change with speed and are uniform across the guide. We ignore the initial stress state of the saw and neglect stresses that could result from thermal effects.

With the above assumptions, it is not difficult to show that the governing equation of the rotating saw in terms of its transverse displacement, $\widetilde{w}(r,\gamma,t)$ becomes [2, 22]:

$$\begin{aligned} &D\nabla^4\tilde{w} + D^*\nabla^4\left(\tilde{w}_{,t} + \Omega\tilde{w}_{,\gamma}\right) \\ &+ \rho h\left\{\tilde{w}_{,tt} + 2\Omega\tilde{w}_{,t\gamma} + \Omega^2\tilde{w}_{,\gamma\gamma}\right\} \\ &- \frac{h}{r}\left\{\left(r\sigma_{rl}\tilde{w}_{,r}\right)_{,r} + \left(\frac{\sigma_{\gamma l}}{r}\tilde{w}_{,\gamma}\right)_{,\gamma}\right\} \\ &= f_r(r,\gamma,t) \end{aligned} \tag{1}$$

wherein the comma-subscript notation signifies partial differentiation, $\rho$ is the mass density, $D = \frac{Eh^3}{12(1-\nu^2)}$ is the flexural rigidity, wherein $E$ is the Young's modulus and $\nu$ is the Poisson's ratio, $D^* = \eta D$ is the internal damping in the saw, wherein $\eta$ is the Kelvin-Voigt damping parameter, $\nabla^4$ is the bi-harmonic operator, and $\sigma_{rl}$, $\sigma_{\gamma l}$ are the in-plane stresses due to rotation and that take the form detailed in [22]. $f_r(r,\gamma,t)$ in Eq. (1) is the uniformly distributed force on the saw that is comprised of forces due to the distributed and lubricated guides, $f_{gr}(r,\gamma,t)$, the lateral regenerative forces due to cutting, $f_{lr}(r,\gamma,t)$, and the process damping force due to workpiece interaction along the lateral direction, $f_p(r,\gamma,t)$.

Since the fluid between the saw and the guide is only modelled as a distributed stiffness, its interaction force can be written as:

$$\begin{aligned} f_{gr}(r,\gamma,t) = \sum_{j=1}^{J}\Big[&\left\{-k_{f_j}\widetilde{w}(r,\gamma,t)\right\} \\ &\left\{H\left(\gamma-\gamma_{1_j}\right) - H\left(\gamma-\gamma_{2_j}\right)\right\} \\ &\left\{H\left(r-r_{1_j}\right) - H\left(r-r_{2_j}\right)\right\}\Big] \end{aligned} \tag{2}$$

wherein $k_{f_j}$ is the uniformly distributed stiffness between the $j^{th}$ guide pad pair and the saw, respectively, which can be written in simplified way as: $k_{f_j} = \frac{E_{f_j}}{h_{f_j}}$, wherein $E_{f_j}$ and $h_{f_j}$ are the stiffness constant and the clearance between the $j^{th}$ guide pad pair and the saw, respectively. Also, $J$ in Eq. (2) is the total number of guide pad pairs and $H(.)$ is the Heaviside function to account for the guides distributed nature.

The lateral regenerative cutting force due that is proportional to relative tooth displacements can be expressed in stationary coordinates as [7, 20]:

$$\begin{aligned} f_{lr}(r,\gamma,t) = -\sum_{i=1}^{N_t}\left(\frac{1}{r}\right)K_r[\widetilde{w}(r,\gamma,t) - \widetilde{w}(r,\gamma,t-T)] \\ \delta(r-r_0)\delta(\gamma-\gamma_i)g(\gamma_i) \end{aligned} \tag{3}$$

wherein $K_r$ is an empirically determined cutting force coefficient, $\delta(.)$ is the dirac delta function, $\gamma_i$ is the instantaneous tooth position which is given by: $\gamma_i = \gamma_{st} + \Omega t + (i-1)\gamma_p, (\gamma_1 = \gamma_{st}$ when $t = 0; \gamma_p$ is the angular pitch), and $g(\gamma_i)$ is a screening function to check the engagement of tooth with a mathematical form as: $g(\gamma_i) = 1$, when $\gamma_{st} < \gamma_i < \gamma_{ex}$, and $g(\gamma_i) = 0$ otherwise. The form of the regenerative force shown in Eq. (3) assumes that the regeneration mechanism is governed only by the present and previous vibrations, i.e., the delay between two vibrations imprinted by successive teeth in cut, and not due to multiple delays.

The other forces are those due to the process damping effect caused by the interference between the saw tooth flank face and the waves left on the machined surface by the previous tooth's vibrations. Process damping is thought to be influenced by the behavior of the workpiece material being cut, by the saw tooth's geometry, the vibration amplitude and wavelength, and their relationship with the vibration frequencies, cutting speeds, tool geometry and tool wear. Modelling these effects is not trivial. We hence follow the usual approach in metal cutting [11–15], wherein the complex interactions are described by an empirically determined process damping force coefficient, $C$. The process damping force with this coefficient takes the form of:

$$\begin{aligned} f_p(r,\gamma,t) = -\sum_{i=1}^{N_t}\left(\frac{1}{r}\right)\left\{C\left(\frac{S}{\Omega r}\right)\widetilde{w}_{,t}(r,\gamma,t)\right\} \\ \delta(r-r_0)\delta(\gamma-\gamma_i)g(\gamma_i). \end{aligned} \tag{4}$$

Since the process damping force is active only for when the tooth is in cut, the $\delta$ function and the screening function, $g$ in Eq. (4) ensure this. Moreover, since process damping is hypothesized to be more pronounced at low speeds, the form of the model in Eq. (4) captures this behavior.

Given that Eq. (1) is a fourth-order partial differential equation solution, the Galerkin's projection method is employed to approximate the solution. The response at the location $(r_0,\gamma_i)$ for a guided saw subjected to lateral regenerative cutting forces and with process damping forces is assumed to be of the same form as it was without these forces, i.e., the response using the modal expansion theorem can be shown to be [2, 22]:

$$\begin{aligned} \widetilde{w}(r_0,\gamma_i,t) = \sum_{m=0}^{M}\sum_{n=0}^{N}\{C_{mn}(t)\cos(n\gamma_i) + S_{mn}(t)\sin(n\gamma_i)\} \\ R_{mn}(r_0). \end{aligned} \tag{5}$$

Equation (5) accounts for only the present response. However, since the solution also requires information about the response at the previous tooth period, that can be written as:

$$\begin{aligned}\widetilde{w}(r_0,\gamma_i,t-T)=\sum_{m=0}^{M}\sum_{n=0}^{N}\{C_{mn}(t-T)\cos(n\gamma_i)\\ +S_{mn}(t-T)\sin(n\gamma_i)\}R_{mn}(r_0)\end{aligned} \tag{6}$$

$M$ and $N$ within Eqs. (5) and (6) represent the number of nodal circles and nodal diameters, respectively, $r_0$ is the radial location of clamped saw's outer free edge and, $C_{mn}(t)$ and $S_{mn}(t)$ are the coefficients to be determined by substituting the assumed response in the governing equation and applying the Galerkin's procedure. $R_{mn}(r)$ is a radial shape function and is taken to be in the form of a polynomial in $r$ as:

$$\begin{aligned}R_{mn}(r)=E^0_{mn}r^m+E^1_{mn}r^{m+1}+E^2_{mn}r^{m+2}+E^3_{mn}r^{m+3}\\ +E^4_{mn}r^{m+4}\end{aligned} \tag{7}$$

wherein $E^p_{mn}$ with $p=0,1,\ldots,4$ are unknowns to be determined from the boundary conditions and displacement normalization condition. The boundary conditions for the saw being clamped at its center and free at its periphery are:

$$\begin{aligned}&\tilde{w}(b,\gamma,t)=\tilde{w}_{,r}(b,\gamma,t)=0,\\ &M_{rr}(a,\gamma,t)=Q_r(a,\gamma,t)-\left(\frac{1}{a}\right)\frac{\partial}{\partial\gamma}\left(M_{r\gamma}(a,\gamma,t)\right)=0\end{aligned} \tag{8}$$

wherein, $M_{rr}, M_{r\gamma}$ are bending moments and $Q_r$ is shear force, respectively.

Substituting the assumed solution i.e., Eqs. (5–8) in the governing equation expression and calling the residue as $L(r,\gamma,t)$, the Galerkin's projection is applied as given below:

$$\int_0^{2\pi}\int_b^a L(r,\gamma,t)\left[R_{ql}(r)\cos(l\gamma)\right]rdrd\gamma=0 \tag{9}$$

$$\int_0^{2\pi}\int_b^a L(r,\gamma,t)\left[R_{ql}(r)\sin(l\gamma)\right]rdrd\gamma=0 \tag{10}$$

wherein $q=0,1,2,\ldots,M, l=0,1,2,\ldots,N$.

Equations (9) and (10) result into a set of coupled differential equations, which when simplified and rewritten in matrix form, become:

$$[\boldsymbol{A}]\{\ddot{\boldsymbol{x}}(t)\}+[\boldsymbol{B}]\{\dot{\boldsymbol{x}}(t)\}+[\boldsymbol{C}]\{\boldsymbol{x}(t)\}=\{\boldsymbol{F}_{lr}(t)\} \tag{11}$$

wherein $[\boldsymbol{A}]$, $[\boldsymbol{B}]$,and $[\boldsymbol{C}]$, represent the mass, gyroscopic/damping, and stiffness matrices, respectively, and include the effect of the fluid force and of the process damping force, and $\{\boldsymbol{F}_{lr}(t)\}$ represents the regenerative forces.

The regenerative cutting force component within $\{\boldsymbol{F}_{\boldsymbol{lr}}(t)\}$ can be estimated by substituting Eqs. (5) and (6) into Eq. (3) and then again applying the Galerkin's procedure and after rearranging terms, the forcing term i.e., $\{\boldsymbol{F}_{\boldsymbol{lr}}(t)\}$ in Eq. (11) can be shown to become:

$$\{\boldsymbol{F}_{\boldsymbol{lr}}(t)\}=-\left(1-e^{-TD}\right)[\boldsymbol{R}(t)]\{\boldsymbol{x}(t)\} \tag{12}$$

wherein $e^{-TD}\{\boldsymbol{x}(t)\}=\{\boldsymbol{x}(t-T)\}$ and $[\boldsymbol{R}(t)]$ is a time dependent matrix related to the cutting forces. Note that $[\boldsymbol{R}(t)]$ is periodic with period $T$, as it is a function of $\gamma_i$ which is periodic with period $T$. Therefore, by substituting $\{\boldsymbol{F}_{\boldsymbol{lr}}(t)\}$ from Eq. (12) into Eq. (11), the final system of governing equations for the guided circular saw coupled with process damping and under the influence of multiple moving regenerative flanks cutting forces can be shown to become:

$$\begin{aligned}&[\boldsymbol{A}]\{\ddot{\boldsymbol{x}}(t)\}+[\boldsymbol{B}]\{\dot{\boldsymbol{x}}(t)\}+[\boldsymbol{C}]\{\boldsymbol{x}(t)\}\\ &\quad+\left(1-e^{-TD}\right)[\boldsymbol{R}(t)]\{\boldsymbol{x}(t)\}\\ &\quad=\{0\}.\end{aligned} \tag{13}$$

As $[\boldsymbol{R}(t)]$ is periodic, it can be written in terms of a Fourier series expansion as:

$$[\boldsymbol{R}(t)]=\frac{1}{2}[\boldsymbol{R}_0]+\sum_{k=1}^{\infty}\{[\boldsymbol{R}_{c_k}]\cos(k\omega t)+[\boldsymbol{R}_{s_k}]\sin(k\omega t)\} \tag{14}$$

wherein, $[\boldsymbol{R}_0]=\frac{2}{T}\int_0^T[\boldsymbol{R}(t)]dt$, $[\boldsymbol{R}_{c_k}]=\frac{2}{T}\int_0^T[\boldsymbol{R}(t)]\cos(k\omega t)dt$, and $[\boldsymbol{R}_{s_k}]=\frac{2}{T}\int_0^T[\boldsymbol{R}(t)]\sin(k\omega t)dt$.

The solution to Eq. (13) with periodic coefficients can be written in Fourier series form with frequency component: $\lambda+ik\omega$ as [20]:

$$\{\boldsymbol{x}(t)\}=\left[\frac{1}{2}\{\boldsymbol{x}_0\}+\sum_{k=1}^{\infty}(\{\boldsymbol{x}_{c_k}\}\cos(k\omega t)+\{\boldsymbol{x}_{s_k}\}\sin(k\omega t))\right]e^{\lambda t} \tag{15}$$

wherein $\{\boldsymbol{x}_0\}$, $\{\boldsymbol{x}_{c_k}\}$, and $\{\boldsymbol{x}_{s_k}\}$ are time independent coefficient vectors, and $\lambda$ is the characteristic variable of the system. Since other prior research has shown that solutions that consider only the average component of the Fourier series are comparable to those solutions that consider higher order terms [20], especially when there are multiple teeth in cut as there are in circular sawing, solutions herein too only retain the average component of the Fourier series in what is otherwise called the zero-order solution. Substituting $[\boldsymbol{R}(t)]$ and $\{\boldsymbol{x}(t)\}$ from Eqs. (14–15) into Eq. (13) and taking only the zero order term results in:

$$\left\{\lambda^2[\boldsymbol{A}] + \lambda[\boldsymbol{B}] + [\boldsymbol{C}] + \frac{1}{2}\left(1 - e^{-T\lambda}\right)[\boldsymbol{R}_0]\right\}\{\boldsymbol{x}_0\} = \{0\}. \tag{16}$$

Equation (16) is a characteristic equation, and because it is nonlinear on account of the exponent that contains the delay term, solving it by reducing it to the standard eigenvalue problem form is not feasible. As such, we instead solve Eq. (16) using the Muller's optimization technique with deflation to obtain the system's eigenvalues, i.e., $\lambda$. The Muller algorithm is a numerical technique for finding complex roots. It is a variation of the secant method, except that instead of using two points to interpolate the curve, it uses three points to construct an interpolating quadratic polynomial. Deflation is a root finding procedure that is used to locate many roots [21]. For details on procedures to solve the characteristic equation using Muller's technique, please refer to the study conducted by Singhania [22]. The resulting eigenvalues are complex valued, wherein the imaginary part corresponds to the natural frequency of the system, and the real part represents the growth or decay. To get a sense of the stability of the guided rotating saw, Eq. (16) is solved for every speed of interest for different workpiece materials, different engagement conditions, different clearances between the guide and the rotating saw, different guide locations, and for characterizing the influence of process damping on regeneration. Results for each of these cases is discussed next.

## 3. Numerical results for the regenerative instability of guided saws

This section presents model-based investigations on regenerative instabilities of a guided saw. To begin with, the model with regenerative instabilities is verified by benchmarking with already published results from the literature [7]. However, since reports in the literature were limited to regenerative instabilities of an unguided saw for a wood cutting application in which there was no process damping, benchmarking is limited to that case. Following verification of the model, for the saw parameters of interest in this work, the verified model is used to characterize critical speed and regenerative instabilities for guided and unguided saws. That characterization is followed by discussions on regenerative instabilities being influenced by different workpiece materials, different engagement conditions, and by different clearances between the guide and the rotating saw. The guide's location influencing regeneration is also discussed. And, finally, the influence of process damping on regeneration is discussed.

### 3.1 *Model verification*

We benchmark our predictions with results from [7]. For parameters given therein, the equations are solved at every speed of interest, and the resulting frequency-speed characteristics are shown in figure 2.

As is evident from comparisons in figure 2, since model-predicted results agree with data extracted from [7], the model is deemed verified. Since circular sawing process is excited by cutting forces at the tooth passing frequency and its higher harmonics, hence, figure 2 shows the natural frequency and real part of eigen values changing as a function of tooth passing frequency, instead of rotational speed. Further, interestingly, as is evident from figure 2, there are multiple regions of tooth passing frequencies at which the real part of the eigenvalue is positive. For the configuration investigated, it is evident that the largest or/primary instability region occurs at speeds where the tooth passing frequency is greater than but less than twice the natural frequency of the mode being excited. Furthermore, because the backward (0,5B) and the forward (0,5F) mode have larger instabilities, their contribution to saw displacement is higher than that of higher frequency backward (0,7B) and/or forward (0,7F) mode. Additionally, as is observed from figure 2b, the primary instability region of higher modes spans a wider speed range than that of lower modes.

The real part becoming positive in this case is unlike the cases discussed in the literature [2] in which the fluid media in between the guide and the rotating saw induces shear stresses on the saw and destabilizes it. The real part becoming positive in this case is due regenerative instabilities. And, since the real part of eigenvalues becomes positive before the onset of the first critical speed, it suggests that stability of metal cutting saws subjected to regenerative forces is limited by regenerative instabilities and not by critical speed related instabilities. This observation is consistent with our preliminary observations reported in [9]. Since the model is deemed verified, and since it suggests that regenerative instabilities are more of a concern than critical speed related ones, and that regenerative instabilities occur at lower speeds than critical, and since metal sawing is a low-speed operation, it is imperative to characterize the role of guides and process damping in potentially stabilizing the process. These investigations are hence presented next.

### 3.2 *Regenerative and critical-speed related instabilities*

This section presents model-based investigations characterizing the critical-speed related and regenerative instabilities for a saw guided with two pairs of guide pads. The saw is assumed to be made of steel with a density of 7850 kg/m$^3$, a modulus of 210 GPa, and a Poisson ratio of

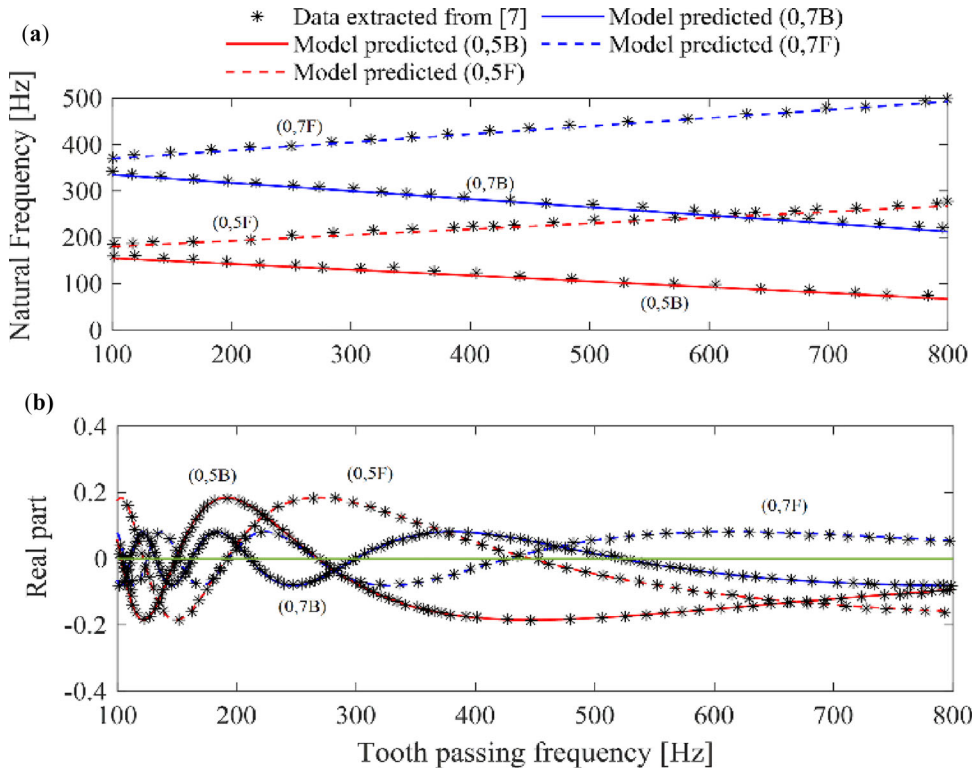


**Figure 2.** Comparisons of model-predicted results with those from the published literature as a way of verifying the proposed model. (**a**) Natural frequencies changing with speed/tooth passing frequency, (**b**) Real part of saw's eigenvalues changing with speed/tooth passing frequency.

0.3. The saw's outer and inner diameters are taken to be 285 mm and 85 mm, respectively, and its thickness is taken to be 2 mm. The internal damping of the saw is set to be $10^{-6}$ sec. The number of teeth is taken as 60. The saw is assumed to be cutting a steel bar of diameter 76 mm at an instantaneous engagement with an entry angle of $\gamma_{st} = 343^\circ$ and an exit angle of $\gamma_{ex} = 17^\circ$ measured along the counterclockwise direction as shown in figure 1. We assume the material being cut to be characterized by a cutting force coefficient of $K_r = 1000$ N/m. The influence of process damping on the stability of saw has been separately discussed in the subsequent sections.

For the guides, the first pair is assumed to be positioned between $\gamma_1 = 25^\circ$ and $\gamma_2 = 55^\circ$, while the second is positioned between $\gamma_3 = 305^\circ$ and $\gamma_4 = 335^\circ$, resulting in a guide pad pair size of $30^\circ$ for each. The guides are placed symmetrically on either side of the cutting zone. This configuration is typical of multiple guides used in industrial metal cutting circular sawing processes. The clearance between the saw and the guides was set to 0.15 mm for this analysis. Only the representative case of oil-lubricated guides is considered herein with the fluid is modelled as being a distributed stiffness with a stiffness constant of $45 \times 10^3 \mathrm{N/m^2}$.

With the above parameters, predicted dynamics are shown in figure 3. And like in figure 2, figure 3 also shows the imaginary and real parts of the eigenvalues of the system changing with tooth passing frequency instead of rotational speed. The tooth passing frequency is a function of speed and number of teeth, i.e., $\Omega \times (N_t/60)$ and is equal to saw's rotational speed in the present case since the number of teeth for the saw under consideration is 60. To differentiate the role of guides, results shown in figure 3 also include those with a saw that is not guided.

As is evident from figure 3, the natural frequencies of a guided saw are higher than that of an unguided saw. The critical speed in the presence of regenerative cutting forces for the guided saw system is 8860 Hz (rpm). This corresponds to a marginal increase ($\sim$ 4%) over the unguided case. Interestingly, lateral regenerative forces appear to have no influence on the critical speed for either the unguided case or the guided case. However, as is evident from the real part of the eigenvalues, regenerative instabilities are influenced by the saw being guided or not. In either case, these instabilities occur at speeds (tooth passing frequencies) lesser than critical speed related ones. For both cases, the first mode to become unstable is the (0,1) backward wave. For a saw that is not guided, the first region of instability occurs in the 200–630 Hz (rpm) range. Within this tooth passing frequency range, the guided saw appears to stabilize cutting at speeds between 225 and 335 Hz (rpm). However, there are several different frequency

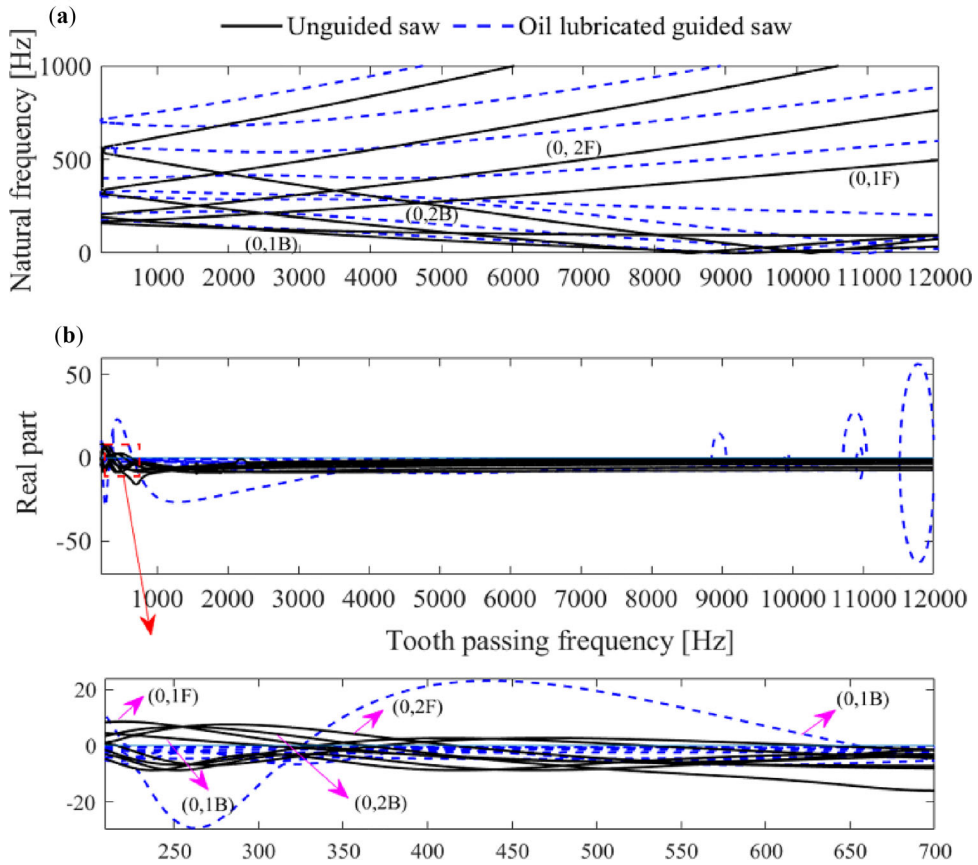


**Figure 3.** Frequency-speed characteristics for a guided and unguided saw subjected to regenerative forces. (**a**) Natural frequency changing with tooth passing frequency, (**b**) Real part of the eigenvalue changing with tooth passing frequency.

(speed) regions for which the real part is positive even for the saw being guided. Curiously, the regenerative instabilities for a guided saw appear to be more severe than those for a saw that is not guided as is evident from the magnitude of the real part that becomes positive. Above observations suggest that there exist local speed pockets of stability. Such information would be useful to guide selection of cutting parameters to operate within these pockets to ensure stable cutting.

The behavior seen in figure 3 is a function of the saw geometry, its material, fluid stiffness properties, workpiece material being cut, and engagement conditions. Parametric analysis to separately characterize the role of the main influencing parameters is discussed next. And, since the real part characterizes system instabilities, discussions in the subsequent sections is limited to showing only how the real part changes for different system parameters.

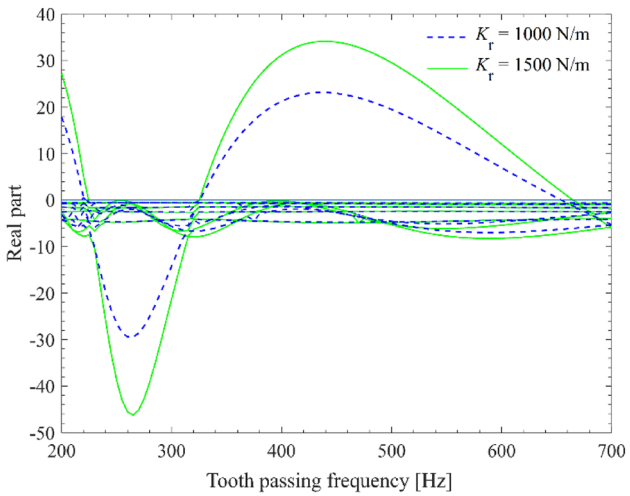


**Figure 4.** Comparative speed-dependent behaviour of the real part of the eigenvalue for different workpiece materials.

### 3.3 *Regenerative instabilities being influenced by material being cut*

This section discusses the influence of the material dependent cutting force coefficient, $K_r$ on the regenerative instabilities of the guided saw. To do so, only $K_r$ is varied at two levels, and all the other parameters are kept the same as listed in the previous subsection. A low level of $K_r$= 1000 N/m corresponds to cutting a soft material such as Aluminium, while a high level of $K_r$= 1500 N/m

corresponds to cutting a relatively difficult-to-cut material such as steel. Results are shown in figure 4.

As is evident from the figure 4, the rate of growth of instability is higher for larger values of cutting force coefficients. The width of the unstable regions remains the same. The mode that becomes unstable for both the cases remains the same (0,1) backward wave. The growth rate of instabilities increasing with $K_r$ is consistent with the earlier reported work on regenerative instabilities in circular sawing [7, 9], even though that analysis was for the case of an unguided and/or a point-guided saw. However, the width of the unstable region remaining unchanged is unlike what is typically observed in other metal cutting processes such as in end milling [20] in which case the widths of instabilities change with changing material-dependent cutting force coefficients. The differences are likely due to the radial and tangential force components contributing to regeneration in end milling processes, whereas in circular sawing, only the lateral component of the force component is important.

### 3.4 *Regenerative instabilities being influenced by engagement conditions*

As the saw progresses through the cut, the engagement conditions and number of active teeth in cut continuously change. The process starts with small engagements. These increase monotonically till a maximum condition that corresponds to the saw being mid-way through the cut, and, then engagement conditions decrease till the end of the cut is reached. To characterize the influence of changing engagement conditions on the regenerative instability of a guided saw, two representative cases are investigated herein. The first is a low engagement condition with a 20° engagement with the bar with the active number of teeth being four. The second condition is with a higher engagement of 34° with a bar with the corresponding active number of teeth being six. Results with these are shown in figure 5. For results shown, all other parameters were kept the same as discussed in the section titled 'Regenerative and critical-speed related instabilities'.

Figure 5 shows that changes in engagement conditions or the number of active teeth in cut have no effect on the regions of instabilities. However, the rate of growth of the instability increases with larger engagements and with higher number of active teeth in cut. These results are also consistent with those reported in [7, 9], even though those observations were obtained without the use of guides or for the case of a point-guide. Widths of instabilities remaining unchanged for changing engagements is unlike what has been reported for end milling processes [20]. Differences in this case too, like in the case of changing cutting coefficients, are thought to be due to regeneration in sawing being influenced only by the lateral force component, and not by tangential and radial components.

### 3.5 *Regenerative instabilities being influenced by clearances*

This subsection discusses how the stability of a guided saw changes with changing the clearance in between the rotating saw and the pairs of distributed guides in the presence of regenerative forces. Results shown in figure 6 are for three representative clearances. Since the fluid's stiffness is modelled to be a function of the clearance, a change in clearance changes the fluid's stiffness, with lesser clearances translating to higher fluid stiffnesses. All other parameters are kept the same as discussed in the section titled 'Regenerative and critical-speed related instabilities'.

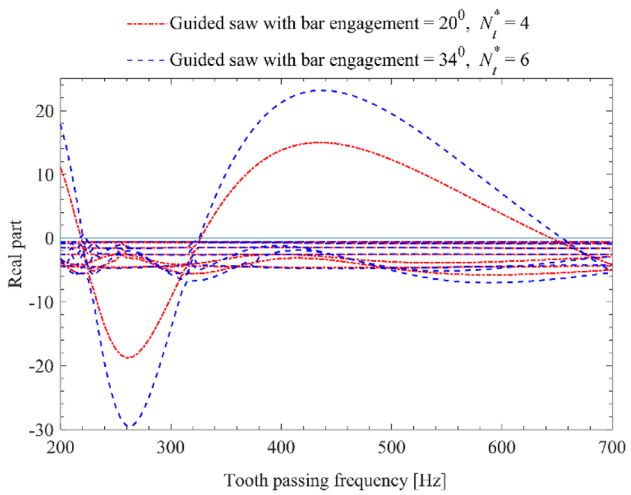


**Figure 5.** Comparative speed-dependent behaviour of the real part of the eigenvalue for different engagements.

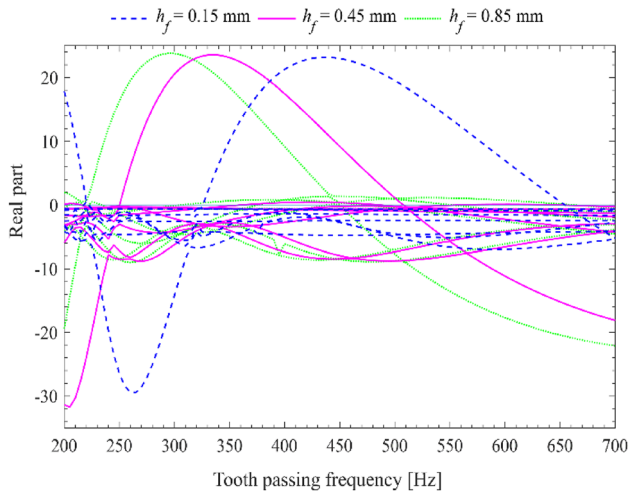


**Figure 6.** Comparative speed-dependent behaviour of the real part of the eigenvalue for different clearances.

As is evident from results in figure 6, a change in the clearance changes the regions of instabilities—as is evident from the real parts of the eigenvalues changing the frequencies and envelopes at which they become positive. There is also a slight change in the width of the unstable envelope for different clearances. Also evident is that for smaller clearances, since the fluid offers more stiffness, there is right shift of the envelope of instabilities to higher frequencies (speeds). The shift in the envelope of instabilities with changing clearances is unlike what was observed for changing cutting force coefficients and/or changing engagement conditions.

These results suggest that is possible to make an otherwise unstable region stable by simply changing the clearance in between the rotating saw and the guides. For example, if cutting must be performed in the speed range of ∼220–300 rpm, the clearance should be minimum. Whereas, if cutting must be performed at relatively higher speeds of 500–700 rpm, then the clearances should be relatively larger. This analysis suggests that it would be useful to design a guided arrangement in which clearances can be adjusted.

### 3.6 *Regenerative instabilities being influenced by the guide's locations*

This section discusses how regenerative stability is influenced by changing the angular location of the pair of guides with respect to the cutting location. For the two guide pad pairs under consideration, the first of which is placed between $\gamma_1 = 25^\circ$ and $\gamma_2 = 55^\circ$, and the second of which is placed between $\gamma_3 = 305^\circ$ and $\gamma_4 = 335^\circ$, the angular location with respect to cutting zone is 8°. This is for the case of the engagement condition being fixed with entry and exit angles of $\gamma_{st} = 343^\circ$ and $\gamma_{ex} = 17^\circ$ respectively as shown in figure 1b. For this engagement condition, the location of the guide pads is changed to result in two other angular locations of 13° and 23°, respectively with respect to the cutting zone. Results for these three angular locations are shown in figure 7. The only change herein is the guide pad's location. All other parameters for analysis herein were kept the same as discussed in the section titled 'Regenerative and critical-speed related instabilities'.

As is evident from figure 7, a change in the angular location of the guides with respect to the cutting zone changes the width and location of the unstable envelopes. For the case of the guides being close to the cutting zone, the unstable envelope occurs at higher tooth passing frequencies (speeds) than when the guides are farther away from the cutting zone. This is thought to be due to the guides being closer to the cutting zone providing more stiffness nearer to the location of the excitation forces. These results suggest that if cutting must be done at specific speeds, and if the cut must be stable, tuning of the guides' angular location with respect to the cutting zone can help stabilize the cutting process. Analysis such as is presented herein is hence useful from the perspective of instructing designing guiding arrangements for stable circular sawing processes—something that was the stated aim of this research.

### 3.7 *Regenerative instabilities being influenced by process damping*

This section discusses the influence of process damping on the dynamics and stability of a guided saw subjected to lateral regenerative cutting forces. Process damping occurs due to interference of the saw's flank face with the previously machined surface that has undulations due to transverse vibrations of saw tooth as it cuts the bar. This is schematically shown in figure 1c. We assume these

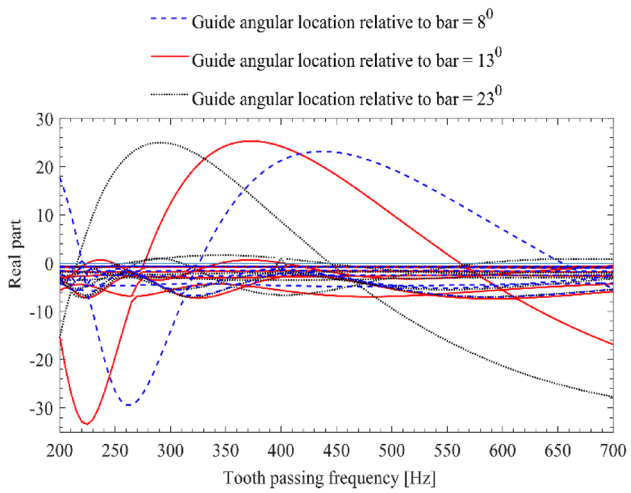


**Figure 7.** Stability being influenced by the guides' angular location with respect to the bar for fixed engagement conditions.

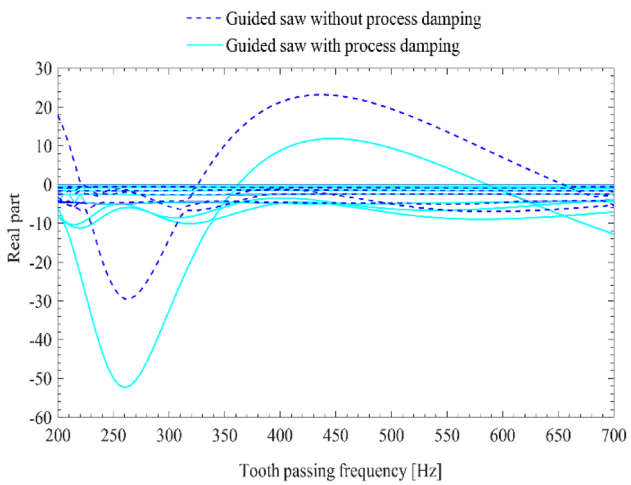


**Figure 8.** Influence of process damping on a guided saw's stability characteristics.

phenomena can be characterized by a process damping coefficient, $C = 10000$ N/m. Though this coefficient must be empirically determined, for cutting of metals such as those of interest herein, such values are typical. We assume the width of cut at the minor cutting edge to be $S = 0.15$ mm, which is typical for worn tools. All other parameters are the same as discussed in the section titled 'Regenerative and critical-speed related instabilities'. With these, the results thus obtained are shown in figure 8. The figure contrasts results for a system with and without process damping.

As is evident from figure 8, process damping plays a role in reducing both the width and the severity of the growth of the instabilities. It also plays a role in stabilizing the process. For example, for a system without process damping, the cut was unstable in the frequency (speed) range of 200 to $\sim$220 Hz, $\sim$300 to $\sim$330 Hz, and $\sim$600 to $\sim$650 Hz. However, for a system with process damping, these speed regions become stable. Since process damping is a naturally occurring phenomena when the tool gets worn, and when there is more contact between the flank face of the saw tooth and the undulations on the machined surface, it is not inherently inimical to the system. This is consistent with reports on the role of process damping in other machining processes.

## 4. Conclusions

The stability characteristics of a guided rotating circular saw under the influence of multiple moving regenerative cutting forces were presented in this paper. Systematic model-based analysis facilitated understanding the role of material being cut, changing engagements, guide placement relative to the saw and the cutting zone, and process damping. The following general conclusions may be drawn from the analysis: (i) Regenerative instabilities are characterized by a growth in the real part of the eigenvalue of the system and that these occur before the onset of critical speeds; (ii) Clearance between the guide and the rotating saw and the guide's circumferential placement with respect to the cutting zone both influence the severity and speed regions of instabilities; (iii) Material being cut and changing cutting engagements do not significantly influence the region of instabilities; (iv) Process damping can help stabilize an otherwise unstable process.

Though there is a need for experimental validation of the model-based observations presented in this work, and though that can form part of future studies, our observations can still instruct the design of stable guided metal sawing processes in industries. For instance, those desiring to cut metal at low speeds, since critical speeds would not limit cutting as much as regenerative instabilities would, practitioners and users of sawing equipment could tune the placement of guides to create pockets of stability to reduce the forced vibration response characteristics.

## Acknowledgment

This research was supported by the Government of India's Science and Engineering Research Board's Early Career Research Award—SERB/ECR/2016/000619. The authors also acknowledge Mr. Anurag Singh for his insightful technical inputs.

### Declarations

**Conflict of interest** On behalf of all authors, the corresponding author states that there is no conflict of interest.

## References

[1] Zhuo R, Deng Z, Chen B, Guoyue L and Bi S 2021 Overview on development of acoustic emission monitoring technology in sawing. *Int. J. Adv. Manuf. Technol.* 116: 1411–1427. https://doi.org/10.1007/s00170-021-07559-5.

[2] Singhania S, Singh A and Law M 2022 Dynamics and stability of metal cutting circular saws with distributed and lubricated guides. *J. Vib. Eng. Technol.* 10: 3119–3131. https://doi.org/10.1007/s42417-022-00544-6.

[3] Altintas Y and Weck M 2004 Chatter stability of metal cutting and grinding. *CIRP Ann. Manuf. Technol.* 53: 619–642. https://doi.org/10.1016/S0007-8506(07)60032-8.

[4] Munoa J, Beudaert X, Dombovari Z, Altintas Y, Budak E, Brecher C and Stepan G 2016 Chatter suppression techniques in metal cutting. *CIRP Ann. Manuf. Technol.* 65: 785–808. https://doi.org/10.1016/j.cirp.2016.06.004.

[5] Altintas Y, Stepan G, Budak E, Schmitz T and Kilic Z M 2020 Chatter stability of machining operations. *J. Manuf. Sci. Eng. Trans. ASME*. https://doi.org/10.1115/1.4047391.

[6] Tian J and Hutton S G 1999 Self-excited vibration in flexible rotating disks subjected to various transverse interactive forces: a general approach. *J. Appl. Mech. Trans. ASME* 66: 800–805. https://doi.org/10.1115/1.2791758.

[7] Tian J F and Hutton S G 2001 Cutting-induced vibration in circular saws. *J. Sound Vib.* 242: 907–922. https://doi.org/10.1006/jsvi.2000.3397.

[8] Zäh M F 1995 Dynamic process model circular saws, PhD thesis.

[9] Singhania S and Law M 2021 Regenerative instabilities of spring-guided circular saws. *Procedia CIRP* 101: 142–145. https://doi.org/10.1016/j.procir.2021.02.017.

[10] Singhania S and Law M 2023 Influence of process damping on the regenerative instability of guided metal circular sawing. *Manuf. Technol. Today* 22: 20–25.

[11] Wallace P W and Andrew C 1965 Machining forces: some effects of tool vibration. *J. Mech. Eng. Sci.* 7: 152–162. https://doi.org/10.1243/jmes_jour_1965_007_023_02.

[12] Tyler C T and Schmitz T L 2013 Analytical process damping stability prediction. *J. Manuf. Process.* 15: 69–76. https://doi.org/10.1016/j.jmapro.2012.11.006.

[13] Eynian M and Altintas Y 2010 Analytical chatter stability of milling with rotating cutter dynamics at process damping speeds. *ASME. J. Manuf. Sci. Eng.* 132: 021012. https://doi.org/10.1115/1.4001251.

[14] Sahu G N, Jain P, Law M and Wahi P 2023 Emulating chatter with process damping in turning using a hardware-in-the-loop simulator. In: *Advances in Forming, Machining and Automation. Lecture Notes in Mechanical Engineering* (eds) Dixit U S, Kanthababu M, Ramesh Babu A and Udhayakumar S, Springer, Singapore. https://doi.org/10.1007/978-981-19-3866-5_22.

[15] Tunc L T and Budak E 2013 Identification and modeling of process damping in milling. *J. Manuf. Sci. Eng.* 135: 1–12. https://doi.org/10.1115/1.4023708.

[16] Tuysuz O and Altintas Y 2019 Analytical modeling of process damping in machining. *J. Manuf. Sci. Eng. Trans. ASME* 141: 1–16. https://doi.org/10.1115/1.4043310.

[17] Schajer G S 1986 Why are guided circular saws more stable than unguided saws? *Holz Als Roh Und Werkst* 44: 465–469. https://doi.org/10.1007/bf02608068.

[18] Khorasany R M H, Panah A M and Hutton S G 2012 Vibration characteristics of guided circular saws: experimental and numerical analyses. *J. Vib. Acoust. Trans. ASME. DOI* 10(1115/1): 4006650.

[19] Singhania S, Kumar P, Gupta S K and Law M 2019 Influence of guides on critical speeds of circular saws. In: *Advances in Computational Methods in Manufacturing. Lecture Notes on Multidisciplinary Industrial Engineering* (eds) Narayanan R, Joshi S and Dixit U, Springer, Singapore. https://doi.org/10.1007/978-981-32-9072-3_45.

[20] Altintaş Y and Budak E 1995 Analytical prediction of stability lobes in milling. *CIRP Ann. Manuf. Technol.* 44: 357–362. https://doi.org/10.1016/S0007-8506(07)62342-7.

[21] Mathews J H 1992 Numerical methods for mathematics, science and engineering. 2nd edn. Prentice-Hall International, Hoboken.

[22] Singhania S 2023 Dynamics and stability of metal cutting circular saws constrained with lubricated guides, Ph.D. thesis, *Indian Institute of Technology Kanpur*, India